

# Three-Dimensional Response of Buried Pipes under Circular Surface Loading

Susan A. Trickey<sup>1</sup> and Ian D. Moore, M.ASCE<sup>2</sup>

**Abstract:** Three-dimensional response of buried pipes under circular surface loading is investigated using the finite-element method. Previous work by Poulos in 1974 is reexamined, considering the longitudinal behavior of pipes under surface loading. Analyses are performed for pipes of varying stiffnesses and embedment depths. When stiff pipes are located close to the ground surface, the burial depth has little impact on the peak deflection. However flexible pipe deflections decrease significantly as embedment depth increases. Not surprisingly, peak moments increase with pipe stiffness and decrease as the pipes become more remote from the ground surface. The comparison of the new results with those of Poulos indicates that his Mindlin solution calculations are somewhat conservative relative to the finite-element solutions for deeply buried pipes, but unconservative at shallow burial.

**DOI:** 10.1061/(ASCE)1090-0241(2007)133:2(219)

**CE Database subject headings:** Three-dimensional analysis; Buried pipes; Finite element method; Loads.

## Introduction

Buried infrastructure such as water and gas supply pipes are subject to surface live loads as a result of vehicle loading and construction of surface facilities. First generation analysis of the problem has been performed by several researchers using Winkler spring models (Jeyapalan and Abdel-Magid 1987; Rajani et al. 1996). The weakness of the Winkler model is its characterization of soil pressure in terms of the absolute pipe displacement (neglecting the impact of rigid body movements of the soil mass), and it neglects interaction through the soil from location to location.

Poulos (1974) examined the problem using what the writers consider a “second generation” approach, modeling the soil as an elastic isotropic continuum using flexibility matrix assembled by integrating the Mindlin equation for vertical displacement due to vertical load acting on a rectangular area within a semiinfinite mass. The pipe was modeled as a thin horizontal strip of length  $L$  and width  $d$ , having a constant flexibility  $EI$  along its length. No account was made of the actual vertical and lateral dimensions of the pipe, and the pipe was modeled without axial stiffness.

The writers are undertaking a three-dimensional finite-element study of water main response following repair with polymer liners, and treated the Poulos solution as a benchmark test (to confirm the effectiveness of mesh and boundary condition choices). During those comparisons, the differences between the second

generation analysis of Poulos and the finite-element procedure with its ability to model the axial stiffness of the pipe and the full three-dimensional nature of the problem were observed. This paper reports the results of this third generation analysis which provides somewhat different magnitudes and trends of maximum pipe deflections and moments.

## Statement of Problem

The case being analyzed is illustrated in Fig. 1, a geometric configuration directly based on Poulos' work. A pipe of diameter  $d$  and length  $L$  is embedded at a depth  $c$  below the surface of a semiinfinite mass. A uniform circular loading of diameter  $d_f=6d$  is located directly above its central vertical axis. The pipe has a flexural stiffness expressed relative to the soil using flexibility factor  $K_r$ , defined by Poulos as follows (while SI units are illustrated here, any set of consistent units would suffice)

$$K_r = \frac{EI}{E_s L^4} \quad (1)$$

Similarly an axial stiffness factor  $K$  is used to represent the axial stiffness of the prismatic pipe relative to the soil it displaces, where  $K$  is defined by the expression

$$K = \frac{EA}{E_s A_0} \quad (2)$$

where  $K_r$ =relative flexibility of the pipeline;  $K$ =relative axial stiffness of the pipe;  $E_s$ =modulus of elasticity of the soil (kPa);  $E$ =modulus of elasticity of the pipe (kPa);  $I$ =moment of inertia of the pipe ( $m^4$ );  $L$ =length of the pipe (m);  $A$ =cross sectional area of the pipe modeled as a prism ( $m^2$ ); and  $A_0$ =area bounded by the outer circumference of the pipe ( $m^2$ ). The larger the values of  $K_r$  and  $K$  the stiffer the pipe is relative to the soil (Poulos 1974; Poulos and Davis 1980).

The soil is assumed to be an ideal linear elastic isotropic material with a constant Young's modulus  $E_s$  and Poisson's ratio  $\nu_s$ . Shear failure is not modeled, nor is any consideration given to

<sup>1</sup>Engineer in training, Golder Associates, Ottawa, ON, Canada.

<sup>2</sup>Canada Research Chair in Infrastructure Engineering, The GeoEngineering Centre, Queens Univ., Kingston, ON, Canada, K7L 3N6. E-mail: moore@civil.queensu.ca

Note. Discussion open until July 1, 2007. Separate discussions must be submitted for individual papers. To extend the closing date by one month, a written request must be filed with the ASCE Managing Editor. The manuscript for this technical note was submitted for review and possible publication on March 16, 2004; approved on December 13, 2004. This technical note is part of the *Journal of Geotechnical and Geoenvironmental Engineering*, Vol. 133, No. 2, February 1, 2007. ©ASCE, ISSN 1090-0241/2007/2-219-223/\$25.00.

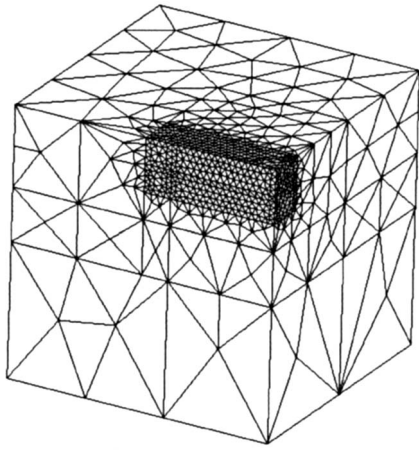


Fig. 1. Finite-element mesh

limiting the contact pressures between the pipe and the soil. The pipe is assumed to be pinned at both ends with moment zero and full restraint against vertical movement. This condition could correspond to a jointed pipe system, where joints only permit limited rotation. Vertical restraint might arise where a pipe segment leaves a manhole being serviced. In any case, this zero moment end condition produces the most conservative values of midpoint deflection and moment.

The Poulos analysis treated the pipe as a thin horizontal strip, with length  $L$ , width  $d$ , and constant flexural rigidity  $EI$ . It does not account for the vertical and lateral dimensions of the pipe, and the pipe was modeled without axial stiffness. In contrast, the finite-element analysis does account for the axial stiffness of the pipe, which is also modeled with both vertical and lateral dimensions (though these dimensions are small relative to the loaded area and pipe length, and are subsequently seen to have no significant effect on the pipe response).

The peak vertical deflection and moment are the main outcomes of the analysis. These occur under the central vertical axis of the loaded area, or midspan along the pipe.

## Finite-Element Model

### Mesh Design

Finite-element package ANSYS 7.1 was used to perform the analyses. The problem was modeled as a linear elastic isotropic, solid material employing ten noded tetrahedral elements.

Specific dimensions and constitutive parameters were selected to reproduce the dimensionless geometry and material conditions considered by Poulos. While any set of properties giving those normalized characteristics would be satisfactory, the approach taken was to select reasonable soil properties and typical pipe geometry, and adjust pipe modulus to provide the correct  $K_r$ :

- First, a pipe diameter of  $d$  was chosen (0.32 m);
- Next, that value of pipe diameter was used to calculate the diameter of the loaded area on the ground surface;
- The  $L/d$  ratio was then used to determine pipe length. Selecting an  $L/d$  ratio of 25, for instance, produces a pipe length of 8 m;
- Modulus of the soil  $E_s$  of 20 MPa was selected;
- For each  $K_r$  value ranging from  $10^{-1}$  to  $10^{-5}$ , the flexural rigidity of the pipe  $EI$  was determined from Eq. (1);
- Pipe thickness  $t$  of 21 mm was selected to give the moment of inertia  $I$  of the pipe; and
- Finally, the modulus of elasticity of the pipe was selected to provide the correct  $EI$ .

Again, it is emphasized that any set of parameters giving the same dimensionless terms  $K_r$ ,  $L/d$ , and  $d_f/d$  could have been employed.

A rectangular elastic solid was constructed, using symmetry and modeling one of the four quarters of the region about the central axis of the pipe and the loaded area above it. Within the solid, the pipe of finite length was located at various normalized

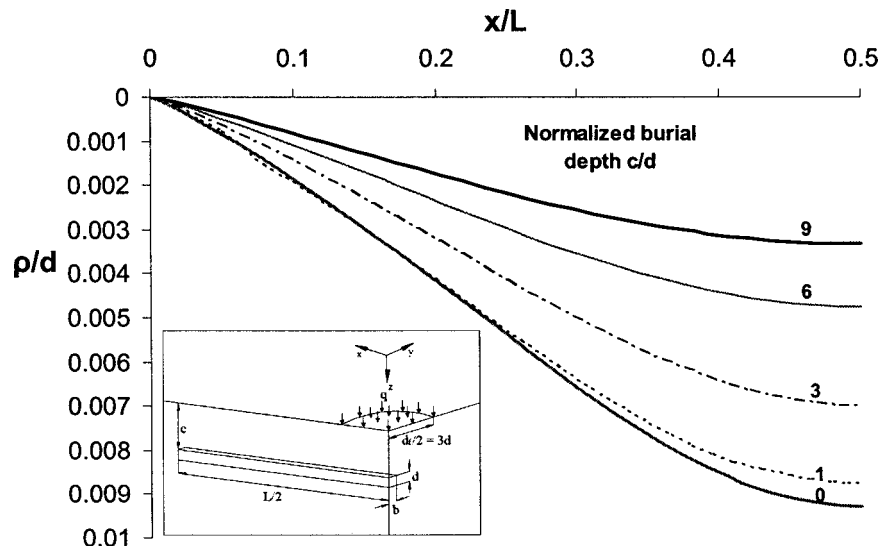
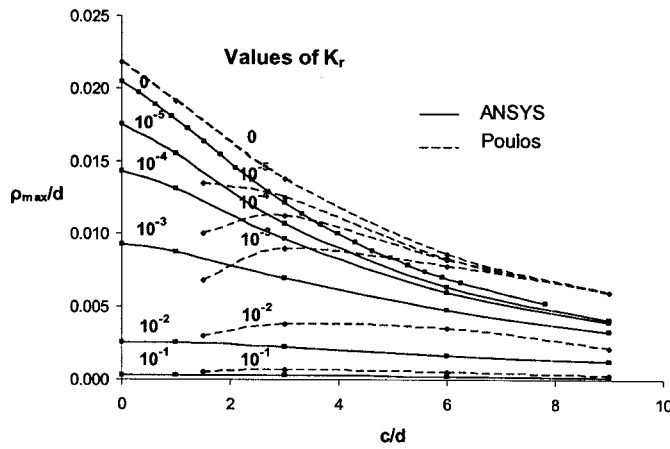
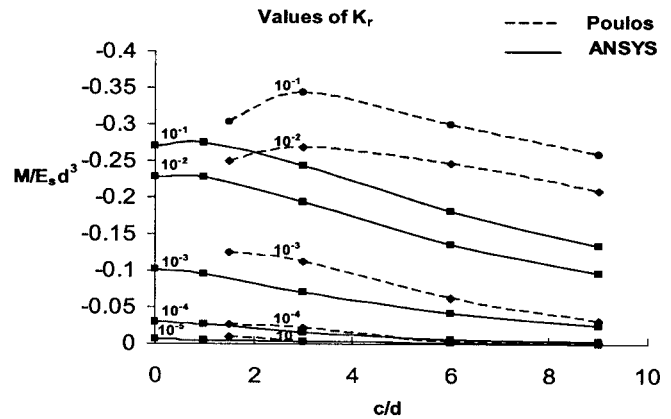


Fig. 2. Deflection profile for pipe beneath circular load:  $K_r=10^{-3}$ ,  $L/d=25$ ,  $\nu_s=0.3$



a: Maximum deflection:  $L/d=25$ ,  $\nu_s=0.3$



b: Central moment  $M$ :  $L/d=25$ ,  $\nu_s=0.3$

Fig. 3. Influence embedment depth: (a) maximum deflection; (b) central moment  $M$

embedment depths  $c/d$  for each particular  $K_r$  value. The pipe was pinned at its ends to simulate Poulos' pipe condition. Figs. 1 and 2 illustrate the typical mesh geometry, for  $c$ , the embedment depth to the top edge of the pipe. The surface pressure was applied to the quarter circle located around the central  $z$  axis of the mesh. The vertical and base boundaries were modeled as smooth and rigid, to prevent horizontal and vertical movement, respectively; the top surface was left unrestrained. A series of different meshes were developed for normalized burial depths ranging from 0 to 9. For a pipe diameter of 0.32 m, this corresponds to a range of burial depths from 0 to just under 3 m (a typical maximum for municipal infrastructure).

### Extent of Mesh Boundaries

Parametric studies were performed to determine the length, width, and depth of the mesh. These analyses were essential to find boundary locations that had minimal impact on the results. The first series of analyses examined the effect of the lower boundary. The second series was undertaken to position the lateral mesh boundaries as described in detail by Trickey (2005). The height and width of the mesh were set to 10 m to ensure a conservative analysis. Selecting lateral boundaries of 10 m provided a mesh width which allowed for the extension of the pipe length in later analyses to examine the effect of pipe length on peak deflections and moments.

### Pipe Modeling

There are various ways the pipe could be modeled using shell, solid, or beam elements. For convenience, the pipe was modeled as a rectangular solid. This method gave the pipe actual physical dimensions, without unnecessarily complicating the mesh. The width  $b$  and depth  $d$  of the pipe were determined by equating half the flexural rigidity  $EI$  determined from the  $K_r$  equation (half the stiffness due to symmetry) to the moment of inertia of a rectangular section multiplied by the pipe modulus

$$\frac{Ebd^3}{12} = \frac{EI}{2} \quad (3)$$

Several pipe widths were investigated to see their effects on the analysis and confirm that the actual dimensions and shape were insignificant. Varying the pipe dimensions had no effect on the

deflections experienced by the pipe provided the flexural rigidity was maintained (Trickey 2005). Analyses were performed which adjusted the width, depth, and modulus of the pipe to maintain  $EI$ , while changing the axial stiffness  $EA$ . These analyses indicated that changing  $EA$  had a negligible effect on calculated pipe response, since the  $K$  value remains high and the pipe is effectively inextensible, when compared to the soil it displaces (e.g., halving the depth increases  $E$  by a factor of eight and an increase of  $K$  and  $EA$  by a factor of four; this had negligible impact on calculated deflections or bending moments). As the Poulos model does not include the axial stiffness of the pipe, differences arise between the finite-element and Poulos solutions for pipe deflections and moments. These will be investigated further in later sections of this paper.

Analyses were also performed to ensure that the decision to model the pipe as a three-dimensional solid yielded results similar to those provided by simple beam theory. Trickey (2005) provides details.

### Soil Modeling

Three-dimensional settlement analysis was performed to verify that the finite-element procedure was able to effectively model the elastic solid. Theoretical stress calculations were performed using Boussinesq's theory for a uniformly loaded circle. Hooke's law was then applied to calculate the strains in the soil. Strain integration theory was then used to calculate the settlement for a 10 m deep semiinfinite mass (Poulos and Davis 1974). The results of this theoretical settlement calculation were then compared to the finite-element results for the  $K_r=0$  case. ( $K_r=0$  is used here to denote the elastic solid without the pipe; it does not correspond to the presence of a pipe of negligible stiffness, i.e., a void with the pipe dimensions.) Both settlement solutions yielded similar results, confirming that the theoretical and finite-element solutions are equivalent (Trickey 2005).

### Deflections

Dimensionless deflection profiles for the pipe are shown in Fig. 3 for a  $K_r$  of  $10^{-3}$  and for various  $c/d$  ratios. It is evident that maximum deflection occurs at the shallowest embedment depth  $c/d=0$ . As the ratio of  $c/d$  increases, the impact of the surface

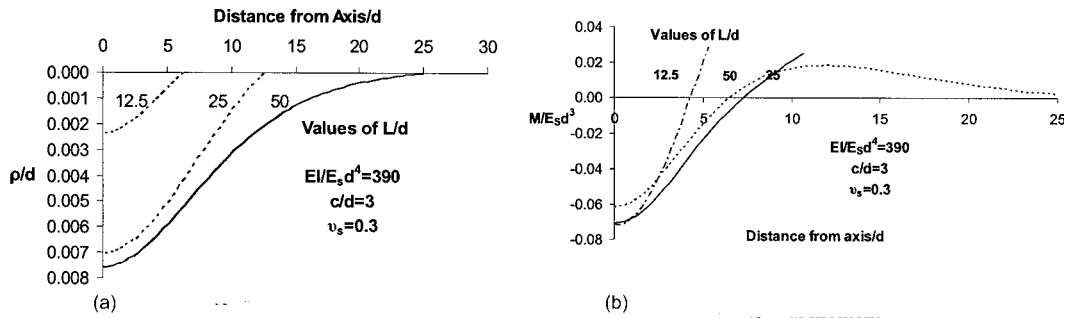


Fig. 4. Influence of length of pipe: (a) deflections; (b) central moment

loading decreases and therefore the deflections decrease. The maximum deflection decreases by a factor of 3 or more as the pipe moves from typical minimum burial depths ( $c/d=2$ ) to maximum depths ( $c/d=9$ ). Similar profiles are observed for  $K_r$  values of  $10^{-1}$ ,  $10^{-2}$ ,  $10^{-4}$ , and  $10^{-5}$  presented in Trickey (2005). These plots differ noticeably from those of Poulos, who found that pipes within the stiffness range of  $10^{-2}$  to  $10^{-4}$  experience maximum deflection at a  $c/d$  ratio of 3. Poulos' model also indicates that pipe deflections at a  $c/d$  ratio of 1.5 fall between those recorded at  $c/d$  of 6 and 9.

Fig. 3(a) demonstrates the variation of maximum deflection of the pipe with embedment depth. Results from both the new finite-element analyses and Poulos' solution are plotted. It is evident that for very stiff pipes ( $K_r$  of  $10^{-1}$  and  $10^{-2}$ ) the deflections are small. Embedment depth has little effect on the maximum deflections for  $c/d$  between 0 and 3. More deeply buried pipes experience even lower deformations. For more flexible pipes, those with stiffnesses between  $10^{-3}$  and  $10^{-5}$ , embedment depth has a significant impact on maximum deflection for shallow and deep burial. As embedment depth increases, maximum deflections decrease. There is however a notable difference between Poulos' results and those resulting from the three-dimensional finite-element analysis. As mentioned earlier, Poulos indicates that pipes with  $10^{-2} \leq K_r \leq 10^{-4}$  reach a deflection peak at a  $c/d$  ratio of from 3 to 5. This trend is not observed in the finite-element results, where deflection peaks when the pipe is at the ground surface ( $c/d=0$ ). For stiffer pipes, the Poulos solution provides, in each case, maximum deflections that were greater than those resulting from the finite-element analysis. For the more flexible pipes, the finite-element analysis provides higher deflections in shallow buried pipelines, and lower deflections in deeper installations.

## Moments

The variation of normalized peak moment with normalized pipe stiffness and embedded depth is shown in Fig. 3(b) for both the finite-element calculations and those reported by Poulos. Not surprisingly, the finite-element analysis produces higher moments for pipes of higher stiffnesses such as  $10^{-1}$  to  $10^{-3}$ . Moments decrease as the flexibility of the pipe increases (as normalized pipe stiffness reaches  $10^{-4}$  and then  $10^{-5}$ ). Moments are negative given the chosen coordinate system. Moment of maximum magnitude generally occurs for the pipe at the ground surface ( $c/d=0$ ). However, the finite-element results do show a slight decrease in moment at a  $c/d$  ratio of 0 for  $K_r$  values of  $10^{-1}$  and  $10^{-2}$ ; this may result from limitations in the discretization and these curves

might also peak at  $c/d=0$  if a more detailed mesh were employed.

As in the case of peak deflections, there are significant differences between the results reported by Poulos and those obtained using the finite-element analysis. Poulos' analyses indicate that for stiff pipes ( $K_r$  of  $10^{-1}$  to  $10^{-2}$ ) peak moments occur at  $c/d$  ratios between 3 and 5, whereas finite-element results mostly produce maximum moments at  $c/d$  of 0. Poulos consistently reports higher moments for both rigid and flexible pipes compared to those obtained using the finite-element analysis. While the Poulos calculation suggests a modest decrease in moment as the burial depth of stiff pipes increases from  $c/d=2$  to 9, the ANSYS solutions imply more dramatic benefits from deeper burial. It appears that by neglecting axial stiffness, the flexural stiffness of the pipe becomes a more important component of the combined soil-pipe stiffness, so greater bending stresses develop (if one of a series of elements acting to resist applied load is removed, the remaining elements carry more).

## Effect of Pipe Length

Poulos examined the effect of pipe length on the maximum pipe deflections. His results indicated that although the length of pipe does affect the deflections away from the center of the pipe, the same maximum deflection occurs regardless of the length. Three different  $L/d$  ratios were examined using finite-element analysis to explore the impact of pipe length on the pipe's maximum deflection and moment. Results are presented in Figs. 4(a and b).

Results indicate that as the  $L/d$  ratio increases the maximum deflection also increases, Fig. 4(a). There is about a 10% difference between the peak deflection of a pipe with a  $L/d$  ratio of 25 and that of 50. Solutions presented earlier in Figs. 2 to 3(a) calculated using a  $L/d$  ratio of 25 are expected to be somewhat lower than those for longer pipes.

The influence of pipe length on the peak moment was also observed. Fig. 4(b) illustrates the results. The finite-element analysis indicates that  $L/d$  ratios of 12.5 and 25 produce similar maximum moments. It also appears that a  $L/d$  ratio of 50 provided lower moments than those observed at ratio of 12.5 and 25. Calculated results for  $L/d=25$  presented earlier in Fig. 3(b) are expected to be conservative relative to those for longer pipe segments.

## Discussion and Conclusions

Finite-element analyses have been conducted to observe the deflections and moments of a pipe embedded in a semiinfinite mass

under circular surface loading. A parametric study was undertaken varying the pipe's stiffness and embedment depth throughout the analyses. Analyses indicated that for relatively stiff pipes, those with flexibility factors  $K_r$  of  $10^{-1}$  and  $10^{-2}$ , the maximum central deflection was not significantly influenced by embedment depth when  $c/d$  falls between 0 and 3. Deflection of flexible pipes, those with flexibility factors from  $10^{-3}$  to  $10^{-5}$ , varied significantly with all values of normalized embedment  $c/d$ . Maximum central deflections and moments occurred when the pipes were buried close to the ground surface, regardless of the relative pipe stiffness.

Comparison of the finite-element calculations with those reported by Poulos revealed some significant differences. Poulos' results for stiff pipes produced deflections and moments that were greater than those observed in the finite-element analyses, yielding more conservative results. For the case of flexible pipes, Poulos' method appears to underestimate maximum deflections for embedment depths less than  $3d$ , and overestimated deflections for embedment depths greater than  $3d$ . Poulos reported central moments that were generally larger than those resulting from the finite-element calculations. The differences observed between the finite-element analyses and those reported by Poulos are believed to be the effect of axial stiffness of the pipe, which the Poulos flexibility method does not consider. Designers of high cost pipe structures vulnerable to surface loading may consider using finite-

element analysis to assess deformations and moments, rather than employing Poulos-type analysis.

## Acknowledgments

This work has been supported by the Natural Sciences and Engineering Research Council of Canada and by the Canadian Government through the Canada Research Chairs Program.

## References

- Jeyapalan, J. K., and Abdel-Magid, B. M. (1987). "Longitudinal stresses and strains in design of RPM pipes." *J. Transp. Eng.*, 113(3), 315–331.
- Poulos, H. G. (1974). "Analysis of longitudinal behavior of buried pipes." *Proc., Conf. on Analysis and Design in Geotechnical Engineering*, ASCE, Austin, Tex., 189–223.
- Poulos, H. G., and Davis, E. H. (1974). *Elastic solutions for soil and rock mechanics*, Wiley, New York.
- Poulos, H. G., and Davis, E. H. (1980). *Pile foundation and design*, Wiley, New York.
- Rajani, B., Zhan, C., and Kuraoka, S. (1996). "Pipe-soil interaction analysis of jointed water mains." *Can. Geotech. J.*, 33, 393–404.
- Trickey, S. A. (2005). "Three-dimensional finite element modeling of buried pipes including frost action." MSc thesis, Dept. of Civil Engineering, Queen's Univ. at Kingston, Canada.